Journal of Bioscience and Bioengineering
VOL. 116 No. 6, 706–715, 2013

www.elsevier.com/locate/jbiosc

Isolation and characterization of a mutant recombinant *Saccharomyces cerevisiae* strain with high efficiency xylose utilization

Masataka Tomitaka,[1] Hisataka Taguchi,[1] Kohsai Fukuda,[1] Takashi Akamatsu,[1,*] and Kenji Kida[2]

Department of Applied Microbial Technology, Faculty of Biotechnology and Life Science, Sojo University, 4-22-1 Ikeda, Kumamoto 860-0082, Japan[1] *and Graduate School of Science and Technology, Kumamoto University, 2-39-1 Kurokami, Chuo-ku, Kumamoto 860-0862, Japan*[2]

Received 12 November 2012; accepted 18 May 2013
Available online 27 June 2013

A recombinant xylose-utilizing *Saccharomyces cerevisiae* strain carrying one copy of heterologous *XYL1* and *XYL2* from *Pichia stipitis* and endogenous *XKS1* under the control of the *TDH3* promoter in the chromosomal DNA was constructed from the industrial haploid yeast strain NAM34-4C, which showed thermotolerance and acid tolerance. The recombinant *S. cerevisiae* strain SCB7 grew in minimal medium containing xylose as the sole carbon source, and its shortest generation time (G_{short}) was 5 h. From this strain, four mutants showing rapid growth (G_{short} = 2.5 h) in the minimal medium were isolated. The mutants carried four mutations that were classified into three linkage groups. Three mutations were dominant and one mutation was recessive to the wild type allele. The recessive mutation was in the *PHO13* gene encoding *para*-nitrophenyl phosphatase. The other mutant genes were not linked to *TAL1* gene encoding transaldolase. When the mutants and their parental strain were used for the batch fermentation in a complex medium at pH 4.0 containing 30 g/L xylose at 35°C with shaking (60 rpm) and an initial cell density (Absorbance at 660 nm) of 1.0, all mutants showed efficient ethanol production and xylose consumption from the early stage of the fermentation culture. In two mutants, within 24 h, 4.8 g/L ethanol was produced, and the ethanol yield was 47%, which was 1.4 times higher than that achieved with the parental strain. The xylose concentration in the medium containing the mutant decreased linearly at a rate of 1 g/L/h until 24 h.

[**Key words:** *Saccharomyces cerevisiae*; Bioethanol; High efficiency of xylose utilization; Spontaneous mutant; Recombinant strain]

Bamboo is a rapidly growing plant on the earth and could be recognized as a lignocellulosic material biomass. The area that is covered by bamboo in Japan has increased to be about twice the size of that of ten years ago. Hence, biomass is preferable for ethanol production and would not compete with food demands. Lignocellulosic biomass is generally a complex mixture of cellulose, hemicellulose, lignin, and small amounts of other compounds, and the ratio of cellulose to hemicellulose in dried bamboo is almost 2:1 (1–5). Native *Saccharomyces cerevisiae* is unable to efficiently use xylose as a sole carbon source and cannot ferment xylose to ethanol despite having a full xylose metabolic pathway (6).

S. cerevisiae takes up xylose by facilitated diffusion (6,7). Facilitated diffusion of xylose occurs through the hexose transporters encoded by the *HXT* (hexose transporter) gene family (8). In *S. cerevisiae*, the hexose transporters with high (*HXT2*, *HXT6*, and *HXT7*) and low (*HXT1*, *HXT3*, and *HXT4*) affinity for glucose are active under low and high glucose conditions, respectively (9–11). High-affinity (*Hxt7* and *Gal2*) and low-affinity (*Hxt4* and *Hxt5*) glucose transporters are required for xylose uptake (12), and xylose uptake through these transporters is significantly less efficient than glucose uptake (13). Also, native *S. cerevisiae* only expresses *Hxt5* and *Hxt7* when xylose is the sole carbon source; thus, these two Hxt proteins are thought to be particularly important for xylose transport (14).

Inside the yeast cell, xylose is converted by a two-step oxidoreductive isomerization to xylulose (15). Xylose is first reduced to xylitol by an NADH-dependent or NADPH-dependent xylose (aldose) reductase (XR) (EC 1.1.1.21). Xylitol is then oxidized to xylulose by NAD-dependent xylitol dehydrogenase (XDH) (EC 1.1.1.14). Xylulose is phosphorylated at the C5–OH position by xylulokinase (XK) to yield xylulose-5-phosphate, which is further channeled into glycolytic intermediates such as glyceraldehyde-3-phosphate and fructose-6-phosphate through the pentose phosphate pathway (PPP). These intermediates are converted to pyruvate in the Embden–Meyerhof–Parnas pathway (16). Under anaerobic conditions, pyruvate is decarboxylated by pyruvate decarboxylase to acetaldehyde, which is then reduced to ethanol by alcohol dehydrogenase.

S. cerevisiae is the preferred microorganism for industrial ethanol production because the yeast produces ethanol with a high yield and specific productivity, has a broad substrate range and high ethanol tolerance, and is tolerant to the inhibitors present in lignocellulosic hydrolysates (17). However, it is unable to effectively use xylose as the sole carbon source (6). Recombinant *S. cerevisiae*

* Corresponding author. Tel.: +81 96 326 3929; fax: +81 96 326 3940.
E-mail addresses: akamatsu@bio.sojo-u.ac.jp, akamatsu@lime.ocn.ne.jp (T. Akamatsu).

1389-1723/$ – see front matter
http://dx.doi.org/10.1016/j.jbiosc.2013.05.027

was constructed by integrating the *Pichia stipitis* genes *XYL1* (encoding the *P. stipitis* xylose reductase) and *XYL2* (encoding the *P. stipitis* xylitol dehydrogenase), and the endogenous *XKS1* (encoding the *S. cerevisiae* xylulokinase). Although the strain was the first to demonstrate aerobic growth on 2% xylose as the sole carbon source (18), ethanol production was very low. Hence, the identification of rate-limiting steps in xylose utilization by *S. cerevisiae* is important with respect to ethanol production. The inability of *S. cerevisiae* to grow on xylose has been attributed to inefficient xylose uptake (19), a redox imbalance generated in the first two steps of xylose metabolism (20), insufficient XK activity, and an inefficient PPP (21). The inability of pentose sugar metabolism to activate the lower part of glycolysis has also been suggested to be the reason for the inability of *S. cerevisiae* to grow on xylose (22,23). To achieve commercially relevant ethanol yields and productivities under high extracellular xylose concentrations, both xylose uptake and metabolism will need to be optimized. Various metabolic engineering efforts involving recombinant *S. cerevisiae* have led to improvements in the initial rate of xylose consumption and xylose transport (24–31). However, ethanol production remained low.

Selective pressure has been successfully employed as an effective method to adapt or evolve *S. cerevisiae* for xylose fermentation. These methods can identify bottlenecks in the xylose metabolic pathway that can then be targeted for genetic engineering. Three separate approaches to adaptation have been applied, with the first two utilizing recombinant *S. cerevisiae* strains and the third a native strain. The first adaptive approach involves growing the recombinant strain in an aerobic environment and gradually adapting the strain to an anaerobic environment (32). The second adaptive approach involves cultivating a recombinant strain on xylose only, switching it to a xylose–glucose mixture, and switching it back again to xylose (33). The third adaptive approach took advantage of the intense selection pressure, under which *S. cerevisiae* mutants showing slow growth on xylose spontaneously arose (34). However, the xylose consumption rate and ethanol production rate remained low. One of the probable reasons for the observations of low consumption and productivity is that a laboratory *S. cerevisiae* strain was used for the analysis.

In this study, we used the industrial, thermotolerant, and acid tolerant *S. cerevisiae* NAM34-4C strain as the parental strain. Next, we constructed a recombinant *S. cerevisiae* strain that assimilated xylose from the parental strain. Then, we isolated and characterized the mutants that demonstrated a high efficiency of xylose assimilation, xylose consumption, and ethanol productivity.

MATERIALS AND METHODS

Microbial strains, plasmids, and oligonucleotides The microbial strains and plasmids used in this study are listed in Table 1. *S. cerevisiae* NAM34-4C was a thermotolerant, acid tolerant yeast, and lactate-assimilating yeast and was used as a parental strain (35). The SCA1 strain carries *MAT***a** and *Δpho87*::*kanMX*, because that the amplicon 3 with the *kanMX* gene in *PHO87* was used for a replacement of *MATα* with *MAT***a** (Table 1). The position of the *kanMX* gene was chosen by an analysis of the nucleotide sequences and gene function adjacent to *MAT***a**. The *Δpho87* did not influence growth rate of the recombinant *S. cerevisiae* strains with xylose utilization. The SCA3 strain was constructed by a series of gene manipulations: (i) transformation of the SCA1 strain with the pZeo plasmid (Table 1), (ii) excision of the *kanMX* region with expression of Cre protein, and (iii) elimination of the pZeo plasmid. pTEF1/Zeo is a 3.6 kb vector that confers resistance to Zeocin in both *Escherichia coli* and yeast strains and carries the DNA structure of P_{TEF}–EM7–*Sh ble*–T_{CYC1}–multiple cloning site–*bla*–*ori*pUC–multiple cloning site (Life Technologies, Tokyo, Japan). The plasmid conferred Zeocin resistance to *E. coli* by the synthetic EM7 bacterial promoter. pSH47 is a 6.8 kb vector that carries the DNA structure of *CEN/ARSH4*–*URA3*–T_{CYC1}–*CRE*–P_{GAL1}–*bla* (36).

The primers (Genenet, Fukuoka, Japan) used in this study were designed using Primer 3 (http://frodo.wi.mit.edu/primer3/) and are listed in Table S1. Sequences of *S. cerevisiae* genes can be found in the *Saccharomyces* Genome Database (http://www.yeastgenome.org/).

Media *S. cerevisiae* strains were grown in yeast extract, peptone, dextrose (YPD) medium (pH 5.5) containing 20 g of peptone, 10 g of yeast extract, and 20 g of glucose per liter of deionized water; this medium was used for routine growth. YPX3 medium was the same as YPD medium except that 30 g/L xylose replaced 20 g/L glucose, and it was used as a batch fermentation medium. YPG medium was the same as YPD medium except that 20 g/L glucose was replaced with 20 g/L galactose, and it was used to induce the Cre recombinase. One liter of MS medium (pH 5.5) contains 5 g of $(NH_4)_2SO_4$ and 1.7 g of yeast nitrogen base without amino acids and ammonium sulfate. MSD, MSX, or MSX3 medium was MS medium containing 20 g/L glucose, 20 g/L xylose, or 30 g/L xylose, respectively. The media were supplemented with adenine (50 mg/L), uracil (50 mg/L), or amino acids (40 mg/L) when necessary. G418 (300 μg/mL) was used to select resistant *S. cerevisiae* cells. Sporulation medium K2 (pH 5.5) contains 10 g of potassium acetate, 1 g of yeast extract, and 0.5 g of glucose per liter. For the preparation of agar medium, 20 g/L of agar was added to the medium. Bacteria were grown in Luria–Bertani (LB) medium (37) or LB agar supplemented with the appropriate antibiotics when necessary. Ampicillin (Ap; 50 μg/mL) and kanamycin (Km; 50 μg/mL) were used to select resistant *E. coli* cells. M9 medium (38) was used as a basal medium for the preparation of competent cells.

Transformation Transformation of *S. cerevisiae* was carried out by the method of Gietz and Woods (39). An aliquot (0.36 mL) of a transformation mixture containing DNA (5 μg) amplified by PCR was added to 0.1 mL (about 10^8 cells) of cell suspension and incubated at 42°C for 40 min. Cells were collected by centrifugation (20,400 ×*g* for 60 s), and the supernatant was discarded. The cells were suspended in 1.0 mL of 2× YPAD medium (pH 5.5) and incubated at 30°C for 4 h. Then, the appropriate aliquots (0.1 mL) were plated onto YPD agar plates containing G418.

DNA manipulation techniques The standard methods for yeast genetics (40) were carried out throughout this work. The preparation of plasmids from *E. coli* was carried out according to the procedure of Birnboim and Doly (41). The manipulation of recombinant DNA was performed with standard techniques as described by Maniatis et al. (38). Restriction enzymes and T4 DNA ligase were from Toyobo (Tokyo, Japan) and were used as recommended by the manufacturer. PCR was performed using KOD FX Polymerase (Toyobo).

DNA sequencing The BigDye Terminator Cycle Sequencing Kit version 3.1 (Applied Biosystems Inc., Tokyo, Japan) was used according to the manufacturer's instructions for DNA sequencing. Results were analyzed on an automated model 3130 Genetic Analyzer (Applied Biosystems Inc.).

Plasmid construction The pZeo plasmid containing *Sh ble* was constructed by modifying plasmid pSH47. The P_{TEF}–EM7–*Sh ble*–T_{CYC1} DNA region (1.2 kb) of pTEF-1/Zeo was amplified using primers F-ZeoPTEF1(ApaI) and R-Zeocyc1TT(KpnI) (Table S1). The amplicons were treated with restriction enzymes *Apa*I and *Kpn*I. The digested DNA was cloned between the *Apa*I and *Kpn*I sites of pSH47 to generate pZeo. When the DNA structure of pZeo was analyzed by PCR and nucleotide sequencing, pZeo (9.3 kb) consisted of pSH47 (6.8 kb), *Sh ble* (1.2 kb), and the *Apa*I–*Kpn*I fragment of pSH47 (1.3 kb).

The marker cassette plasmid, pBlu-LTKTL-TDH3, was used for introducing the *kanMX* or *kanMX-TDH3* promoter DNA fragment into the chromosomal DNA of *S. cerevisiae*. The *TDH3* promoter DNA of *S. cerevisiae* S288C was amplified using primers TDH3-F3 and TDH3-R2 (Table S1). The 1010-bp amplicons were treated with restriction enzymes and cloned between the *Eco*RI and *Pst*I sites of pBluescript II KS+ (42) to generate pBlu-TDH3. The 1609-bp fragment of *loxP*–P_{TEF}–*kanMX*–T_{TEF}–*loxP* derived from *S. cerevisiae* SH6710 was cloned into the *Eco*RI site of pBlu-TDH3 to generate pBlu-LTKTL-TDH3.

The pKX1X2XKS plasmid carrying the *kanMX* marker and xylose-assimilating genes (*XYL1*, *XYL2*, and *XKS1*) was constructed (Fig. S1). pXR was pBluescript II KS+ with P_{TDH3}–*XYL1*–T_{TDH3} DNA. The *XYL1* region of *S. cerevisiae* KF7M was amplified using primers F-GAPDHp(ApaI) and R-XDH3 (Table S1). The amplicons were treated with restriction enzymes and cloned between the *Apa*I and *Xho*I sites of pBluescript II KS+ to generate pXR. pXDH was pBluescript II KS+ with P_{TDH3}–*XYL2*–T_{TDH3} DNA. The *XYL2* region of *S. cerevisiae* KF7M was amplified using primers F-XR3 and R-XK3 (Table S1). The amplicons were treated with restriction enzymes and cloned between *Xho*I and *Eco*52I sites of pBluescript II KS+ to generate pXDH. pXK was pBluescript II KS+ with P_{TDH3}–*XKS1*–T_{TDH3} DNA. The *XKS1* region of *S. cerevisiae* KF7M was amplified using primers F-XDH3 and R-GAPDHt(URA+SacII) (Table S1). The amplicons were treated with restriction enzymes and cloned between the *Eco*52I and *Sac*II sites of pBluescript II KS+ to generate pXK. The P_{TEF}–*loxP*–*kanMX*–*loxP*–T_{TEF} region, the *XYL1* region, and the *XYL2* region were assembled into pXK, which was digested with *Apa*I and *Eco*52I restriction enzymes, as follows: (i) The *kanMX* of pBlu–LTKTL–TDH3 was amplified using primers F-LTKTL(URA+ApaI) and R-LTKTL(Apa1) (Table S1) and treated with *Apa*I restriction enzyme. (ii) The *XYL1* region was amplified using primers M13Rev and –21M13 (Table S1) and treated with *Apa*I and *Xho*I restriction enzymes. (iii) The *XYL2* region was amplified using primers M13Rev and –21M13 and treated with *Xho*I and *Eco*52I restriction enzymes. (iv) The four DNA fragments were ligated to generate pKX1X2XKS.

Construction of *S. cerevisiae* carrying xylose-assimilating *XYL1*, *XYL2*, and *XKS1* genes The *loxP*–P_{TEF}–*kanMX*–T_{TEF}–*loxP*–P_{TDH3}–*XYL1*–T_{TDH3}–P_{TDH3}–*XYL2*–T_{TDH3}–P_{TDH3}–*XKS1*–T_{TDH3} region of pKX1X2XKS was amplified using primers

TABLE 1. Microbial strains and plasmids used in this study.

Bacterial strain	Genotype or phenotype	Reference, source or derivation
Saccharomyces cerevisiae		
NAM34-4C	*MATα*	35
NAM201	*MATα ura3*::*kanMX*	Tfm (NAM34-4C: *kanMX* DNA, G418-r),[a] The *kanMX* DNA was the amplicon 1
NAM203	*MATα leu2Δ*::*kanMX*	Tfm (NAM34-4C: *kanMX* DNA, G418-r). The *kanMX* DNA was the amplicon 2
NAM34-4CG2	*MATα*	Haploid (NAM201 × NAM203)[b]
NAM300	*MATα*/*MAT**a*** *pho87Δ*::*kanMX*	Tfm (NAM34-4CG2: *pho87*::*kanMX* DNA, G418-r) The *pho87*::*kanMX* DNA was the amplicon 3
SCA1	*MAT**a*** *pho87Δ*::*kanMX*	A haploid strain obtained from the tetrads which was constructed from the NAM300 diploid
SCA2	*MATα*	A haploid strain obtained from the tetrads which was constructed from the NAM300 diploid
SCA3	*MAT**a*** *pho87Δ*	SCA1 with deletion of the *kanMX* region
S288C	*MAT**a*** *SUC2 mal mel gal2 CUP1 flo1 flo8-1 SSD1-v1*	YGRC[c]
SH6710	*MATα ho dse2*::*kanMX sed1*::*Sh ble his3Δ1 leu2Δ0 ura3Δ0 lys2Δ0*	YGRC
SCB4	*MAT**a*** *pho87Δ ura3Δ*::XM_2[d]	Tfm (SCA3: XM[d] DNA, G418-r)
SCB5	*MAT**a*** *pho87Δ ura3Δ*::XM_3[e]	Tfm (SCA3: XM DNA, G418-r)
SCB6	*MAT**a*** *pho87Δ ura3Δ*::XM_7[d]	Tfm (SCA3: XM DNA, G418-r)
SCB7	*MAT**a*** *pho87Δ ura3Δ*::XM_8[d]	Tfm (SCA3: XM DNA, G418-r)
SCB11-6B	*MATα ura3Δ*::XM_8	Haploid (SCA2 × SCB7)
SCB11-8A	*MATα ura3Δ*::XM_8	Haploid (SCA2 × SCB7)
SCB11-8C	*MATα ura3Δ*::XM_8	Haploid (SCA2 × SCB7)
SCB101	*MATα*/*MAT**a*** *pho87Δ*	Diploid (SCA2 × SCA3)[f]
SCB101-7C	*MATα*	Haploid (SCA2 × SCA3)
SCB101-2B	*MAT**a*** *pho87Δ*	Haploid (SCA2 × SCA3)
SCB102	*MATα*/*MAT**a*** *pho87Δ*	Diploid (SCB101-7C × SCB101-2B)
SCB102-3D	*MAT**a*** *pho87Δ*	Haploid (SCB101-7C × SCB101-2B)
SCB103	*MATα ura3Δ*::XM_8/*MAT**a*** *pho87Δ*	Diploid (SCB11-8C × SCB102-3D)
SCB103-5B	*MAT**a*** *pho87Δ ura3Δ*::XM_8	Haploid (SCB11-8C × SCB102-3D)
SCB103-10D	*MATα ura3Δ*::XM_8	Haploid (SCB11-8C × SCB102-3D)
SCB13	*MAT**a*** *pho87Δ ura3Δ*::XM_8 $hex3_{1-5}$	Spontaneously isolated hex_{1-5} mutant obtained from SCB7
SCB14	*MAT**a*** *pho87Δ ura3Δ*::XM_8 $HEX1_{2-2}$	Spontaneously isolated HEX_{2-2} mutant obtained from SCB7
SCB15	*MAT**a*** *pho87Δ ura3Δ*::XM_8 $HEX2_{2-3}$	Spontaneously isolated HEX_{2-3} mutant obtained from SCB7
SCB16	*MAT**a*** *pho87Δ ura3Δ*::XM_8 $HEX1_{2-9}$	Spontaneously isolated HEX_{2-9} mutant obtained from SCB7
KF7M	*MAT**a***/*MATα HO/HO trp1/trp1*::P_{TEF}-*ERG25* P_{TDH3}/P_{TDH3}::P_{TDH3}/P_{TDH3}::P_{TDH3}–*BGL1*–*TRP1 ura3/ura3*::*URA3*–P_{TDH3}–*XYL1*–T_{TDH3}–P_{TDH3}–*XYL2*–T_{TDH3}–P_{TDH3}–*XKS1*–T_{TDH3}	A. Kondo,[g] a derivative of the G418-resistant transformant of *S. cerevisiae* KF7 with pIUX1X2XK DNA, 50
SCB104	*MAT**a*** *pho87Δ ura3Δ*::XM_8 $hex3_{1-5}$/*MATα ura3Δ*::XM_8	Diploid (SCB13 × SCB103-10D)
SCB104-7B	*MAT**a*** *pho87Δura3Δ*::XM_8 $hex3_{1-5}$	Haploid (SCB13 × SCB103-10D)
SCB104-5D	*MATα pho87Δ ura3Δ*::XM_8 $hex3_{1-5}$	Haploid (SCB13 × SCB103-10D)
SCB104-2B	*MATα pho87Δ ura3Δ*::XM_8 $hex3_{1-5}$	Haploid (SCB13 × SCB103-10D)
SCB105	*MAT**a*** *pho87Δ ura3Δ*::XM_8 $HEX1_{2-2}$/*MATα ura3Δ*::XM_8	Diploid (SCB14 × SCB103-10D)
SCB105-3B	*MAT**a*** *ura3Δ*::XM_8 $HEX1_{2-2}$	Haploid (SCB14 × SCB103-10D)
SCB105-3A	*MATα ura3Δ*::XM_8 $HEX1_{2-2}$	Haploid (SCB14 × SCB103-10D)
SCB105-7A	*MATα ura3Δ*::XM_8 $HEX1_{2-2}$	Haploid (SCB14 × SCB103-10D)
SCB106	*MAT**a*** *pho87Δ ura3*::XM_8 $HEX2_{2-3}$/*MATα ura3Δ*::XM_8	Diploid (SCB15 × SCB103-10D)
SCB106-8D	*MAT**a*** *pho87Δ ura3Δ*::XM_8 $HEX2_{2-3}$	Haploid (SCB15 × SCB103-10D)
SCB106-1D	*MATα ura3Δ*::XM_8 $HEX2_{2-3}$	Haploid (SCB15 × SCB103-10D)
SCB107	*MAT**a*** *pho87Δ ura3Δ*::XM_8 $HEX1_{2-9}$/*MATα ura3Δ*::XM_8	Diploid (SCB16 × SCB103-10D)
SCB107-5C	*MAT**a*** *pho87Δ ura3Δ*::XM_8 $HEX1_{2-9}$	Haploid (SCB16 × SCB103-10D)
SCB107-8D	*MATα ura3Δ*::XM_8 $HEX1_{2-9}$	Haploid (SCB16 × SCB103-10D)
SCB108	*MAT**a*** *pho87Δ ura3Δ*::XM_8 $hex3_{1-5}$/*MATα ura3*::XM_8 $hex3_{1-5}$	Diploid (SCB104-7B × SCB104-5D)
SCB109	*MAT**a*** *pho87Δ ura3Δ*::XM_8 $HEX1_{2-2}$/*MATα ura3Δ*::XM_8 $HEX1_{2-2}$	Diploid (SCB105-3B × SCB105-3A)
SCB110	*MAT**a*** *pho87Δ ura3Δ*::XM_8 $HEX2_{2-3}$/*MATα ura3Δ*::XM_8 $HEX2_{2-3}$	Diploid (SCB106-8D × SCB106-1D)
SCB111	*MAT**a*** *pho87Δ ura3Δ*::XM_8 $HEX1_{2-9}$/*MATα ura3Δ*::XM_8 $HEX1_{2-9}$	Diploid (SCB107-5C × SCB107-8D)
SCB112	*MAT**a*** *pho87Δ ura3Δ*::XM_8/*MATα ura3Δ*::XM_8	Diploid (SCB103-5B × SCB103-10D)
SCB113	*MAT**a*** *pho87Δ ura3Δ*::XM_8 $HEX1_{2-9}$/*MATα ura3Δ*::XM_8 $HEX1_{2-2}$	Diploid (SCB107-8D × SCB105-3A)
SCB114	*MAT**a*** *pho87Δ ura3Δ*::XM_8 $HEX2_{2-3}$/*MATα ura3Δ*::XM_8 $HEX1_{2-2}$	Diploid (SCB106-8D × SCB105-3A)
SCB115	*MAT**a*** *pho87Δ ura3Δ*::XM_8 $hex3_{1-5}$/*MATα ura3Δ*::XM_8 $HEX1_{2-2}$	Diploid (SCB104-7B × SCB105-3A)
SCB116	*MAT**a*** *pho87Δ ura3*::XM_8 $hex3_{1-5}$/*MATα ura3Δ*::XM_8 $HEX2_{2-3}$	Diploid (SCB104-7B × SCB106-1D)
SCB38	*MAT**a*** *pho87Δ URA3*::XM_8 $HEX1_{2-2}$	Tfm (SCB14: *URA3* DNA, URA^+, G418-s)
SCC2-11B	*MAT**a*** *pho87Δ URA3*::XM_8	Haploid (SCB38 × SCB103-10D)
SCB44	*MAT**a*** *pho87Δ URA3*::XM_8 P_{TAL1}::*kanMX*-P_{TDH3}-*TAL1*	Tfm (SCC2-11B: *kanMX* DNA, G418-r). The *kanMX* DNA was amplified using primers 17 and 18 (Table S1) and pBlu-LTKTL
SCB45	*MAT**a*** *pho87Δ URA3*::XM_8 *pho13Δ*::*kanMX*	Tfm (SCC2-11B: *kanMX* DNA, G418-r). The *kanMX* DNA was amplified using primers 15 and 16 (Table S1) and pBlu-LTKTL
SCB52	*MAT**a*** *pho87Δ URA3*::XM_8 *pho13Δ*::*kanMX*/*MATα ura3Δ*::XM_8	Diploid (SCB45 × SCB103-10D)
SCB52-1B	*MATα URA3*::XM_8 *pho13Δ*::*kanMX*	Haploid (SCB52 × SCB103-10D)
SCB53	*MAT**a*** *pho87Δ URA3*::XM_8 *pho13Δ*::*kanMX*/*MATα**URA3***::XM_8 *pho13Δ*::*kanMX*	Diploid (SCB45 × SCB52-1B)
SCB49	*MAT**a*** *pho87Δ URA3*::XM_8 *pho13Δ*::*kanMX*/*MATα pho87Δ ura3Δ*::XM_8 $hex3_{1-5}$	Diploid (SCB45 × SCB104-2B)
SCB47	*MAT**a*** *pho87Δ URA3*::XM_8 P_{TAL1}::*kanMX*-P_{TDH3}-*TAL1*/*MATα ura3Δ*::XM_8 $HEX1_{2-2}$	Diploid (SCB44 × SCB105-7A)
SCB48	*MAT**a*** *pho87Δ URA3*::XM_8 P_{TAL1}::*kanMX*-P_{TDH3}-*TAL1*/*MATα ura3Δ*::XM_8 $HEX1_{2-3}$	Diploid (SCB44 × SCB106-1D)

Table 1 (*continued*)

Bacterial strain	Genotype or phenotype	Reference, source or derivation
Escherichia coli		
DH10B	*F⁻ mcrA Δ(mrr⁻ hsdRMS mcrBC) Φ80 lacZΔM15 ΔlacX74 recA1 endA1 araD139 Δ(ara leu)7697 galU galK λ⁻ rpsL nupG*)	Life Technologies, 37
Plasmid and amplicon DNA		
pBluescript II KS+	*bla*	42
pBlu-TDH3	*TDH3* promoter (P_{TDH3})	In this study
pBlu-LTKTL-TDH3	*loxP*–P_{TEF}–*kanMX*–T_{TEF}–*loxP*–P_{TDH3}	In this study
pXR	P_{TDH3}–*XYL1*–T_{TDH3}	In this study
pXDH	P_{TDH3}–*XYL2*–T_{TDH3}	In this study
pXK	P_{TDH3}–*XKS1*–T_{TDH3}	In this study
pKX1X2XKS	*loxP*–P_{TEF}–*kanMX*–T_{TEF}–*loxP*–P_{TDH3}–*XYL1*–T_{TDH3}–P_{TDH3}–*XYL2*–T_{TDH3}–P_{TDH3}–*XKS1*–T_{TDH3}	In this study
pSH47	*CEN6/ARSH4 URA3* P_{GAL1} *CRE* TER_{CYC1} *bla* ori_{pUC}	6.8 kb, 37
pTEF1/Zeo	P_{TEF1} *EM7 Sh ble* TER_{CYC1} *bla* ori_{pUC}	Life Technologies
pZeo	*CEN6/ARSH4 URA3* P_{GAL1} *CRE* TER_{CYC1} *bla* ori_{pUC} P_{TEF1} *EM7 Sh ble* TER_{CYC1}	In this study
Amplicon 1	*ura3′*–*loxP*–P_{TEF}–*kanMX*–T_{TEF}–*loxP*–*′ura3*	In this study
Amplicon 2	*leu2′*–*loxP*–P_{TEF}–*kanMX*–T_{TEF}–*loxP*–*′leu2*	In this study
Amplicon 3	*pho87′*–*loxP*–P_{TEF}–*kanMX*–T_{TEF}–*loxP*–*BUD5*–*MAT**a***–*′taf2*	In this study
XM_8	*loxP*–P_{TEF}–*kanMX*–T_{TEF}–*loxP*–P_{TDH3}–*XYL1*–T_{TDH3}–P_{TDH3}–*XYL2*–T_{TDH3}–P_{TDH3}–*XKS1*–T_{TDH3}	In this study
XM_3	*loxP*–P_{TEF}–*kanMX*–T_{TEF}–*loxP*–P_{TDH3}–*XYL1*–T_{TDH3}–P_{TDH3}–*XYL2*–T_{TDH3}	In this study

[a] Tfm, transformation; Tfm (NAM34-4C: *kanMX* DNA, G418-r) indicates G418-r transformants of NAM34-4C with *kanMX* DNA. The flanking region of the *kanMX* DNA contained 40 bp of homology with the replaced DNA region.
[b] Haploid (NAM201 × NAM203) indicates one of the four spores of a single tetrad obtained from the cross between the strains NAM201 and NAM203.
[c] YGRC, Yeast Genetic Resource Center.
[d] XM, XM_2, XM_7, and XM_8 were the DNA fragments carrying the genetic structure of *loxP*–P_{TEF}–*kanMX*–T_{TEF}–*loxP*–P_{TDH3}–*XYL1*–T_{TDH3}–P_{TDH3}–*XYL2*–T_{TDH3}–P_{TDH3}–*XKS1*–T_{TDH3}, including *loxP*, *TEF* promoter, *kanMX* gene, *TEF* terminator, *loxP*, *TDH3* promoter, and *TDH3* terminator.
[e] XM_3 was the DNA carrying the genetic structure of *loxP*–P_{TEF}–*kanMX*–T_{TEF}–*loxP*–P_{TDH3}–*XYL1*–T_{TDH3}–P_{TDH3}–*XYL2*–T_{TDH3}.
[f] Diploid (SCA2 × SCA3) indicates a diploid obtained from the cross between the strains SCA2 and SCA3.
[g] Department of Chemical Science and Engineering, Graduate School of Engineering, Kobe University, Kobe, Japan.

F-LTKTL(URA+ApaI) and R-GAPDHt(URA+SacII) (Table S1). Then, the G418-resistant (G418-r) transformants of *S. cerevisiae* SCA3 with the amplified DNA were selected. Because the flanking region of the two primers contained the *ura3* gene, the G418-r transformants showed the Ura⁻ phenotype.

Analysis of cell growth using a bio-photorecorder The tested strains of *S. cerevisiae* were cultivated on YPD plates overnight at 30°C, inoculated into 10 mL of YPD medium, and cultivated for 24 h at 30°C with shaking (120 reciprocal shaking/min and 4 cm strokes: 120 rpm). The cells were collected by centrifugation at 2400 ×*g* for 1 min at 4°C and suspended in sterilized water. The cell suspension was inoculated into 5 mL of MSX medium in a 5-mL L-shaped test tube or 50 mL of MSX medium in a 500-mL Erlenmeyer flask to give an initial absorbance at 660 nm (A_{660}) = 0.014. The cell density of the 5-mL or 50-mL culture was automatically monitored with a bio-photorecorder (TVS062CA; Advantec Toyo Kaisha, Ltd., Tokyo, Japan) or with a photorecorder (U-2900; Hitachi, Tokyo, Japan), respectively and analyzed for the generation time.

Rescue of the *kanMX* marker To use the G418 selection repeatedly for several gene disruptions in one strain, the *kanMX* marker was removed as described by Güldener et al. (36). The strain containing the *loxP*–*kanMX*–*loxP* cassette was transformed with the *cre* expression plasmid pZeo, which carries the *Sh ble* marker gene and the *cre* gene under the control of the inducible *GAL1* promoter. Expression of the Cre recombinase was induced by shifting cells from YPD to YPG medium. After growth for 1 h in galactose medium, the cells were plated on YPD agar medium and incubated for 1 day at 30°C. The correct loss of the *kanMX* marker gene was verified by diagnostic plating and PCR. The *cre* expression plasmid was removed from the strain by cultivating the strain in YPD medium and plating it on YPD agar plate, and the removal was verified by diagnostic plating and PCR.

Isolation of mutants showing high efficiency of xylose assimilation *S. cerevisiae* SCB7 cells that were cultivated in 10 mL of YPD medium for 24 h at 30°C with shaking (120 rpm) were collected by centrifugation at 2400 ×*g* for 1 min at 4°C and suspended in sterilized distilled water. The cell suspension was inoculated into 5 mL of MSX medium containing uracil in a 5-mL L-shaped test tube to give an initial A_{660} = 0.014. The cell density of the 5-mL culture was automatically monitored with the bio-photorecorder and analyzed for growth. When the cell density abruptly increased, the cell suspension was plated onto an MSX plate and incubated at 30°C for 2–3 days. Large colonies were picked. After isolation of single colonies by streaking cells on YPD plates or by a micromanipulator (Singer MSM systems series 400, Minerva Tech K.K., Tokyo, Japan), the cell growth was monitored and analyzed with the bio-photorecorder. Thus, the mutants showing rapid growth in MSX medium were isolated. One mutant was obtained from independent L-shaped test tubes to provide assurance that each mutant was independently isolated.

Batch fermentation The tested strains of *S. cerevisiae* were grown on YPD agar plates overnight at 30°C, inoculated into 50 mL of YPD medium (pH 4.0), and incubated with shaking (120 rpm) for 24 h at 30°C. From the cell suspension, 1 mL was inoculated into 50 mL of YPX3 medium to give an initial A_{660} = 1.0 and shaken for 48 h at 35°C. To determine the concentrations of ethanol and glucose in the fermentation medium, the supernatant was obtained by centrifugation at 20,400 ×*g* at 4°C for 5 min.

Analysis of glucose, xylose, and ethanol Glucose, xylose and ethanol concentrations of the supernatant were measured using a four-channel biosensor BF7M (Oji Scientific Instruments, Hyogo, Japan) equipped with an automatic liquid sampler BF30ASX, hydrogen peroxide electrode, and planar detection system. The enzymes of the biosensor were glucose oxidase (EC 1.1.3.4), pyranose oxidase (EC 1.1.3.10), and alcohol oxidase (EC 1.1.3.13) for glucose, xylose, and ethanol. The resultant hydrogen peroxide was electrolyzed with a platinum electrode, and the change in currency was detected by the detection system. The ethanol yield (%) was defined as the ratio (%) of the produced ethanol concentration (g/L) to the theoretical maximal ethanol concentration (g/L)[0.51 × initial D-xylose concentration (g/L)].

RESULTS

Construction of *S. cerevisiae* SCB7 with xylose utilization The SCA3 strain was used as a parental strain for constructing the SCB7 strain, which could assimilate xylose. The *XYL1* and *XYL2* genes of *P. stipitis* and *XKS1* of the pKX1X2XKS were amplified using primers F-LTKTL(URA+ApaI) and R-GAPDHt(URA+SacII) (Table S1). Then, G418-r transformants of the strain SCA3 with the DNA of amplicon 3 (Table 1) were isolated to yield strains SCB4, SCB5, SCB6, and SCB7. The xylose assimilation of these four strains and their parental strain (SCA3) was analyzed by cultivating the cells in 5 mL of MSX medium (pH 5.5) containing 20 g/L xylose as the sole carbon source at 35°C. Remarkable efficient growth was observed for three of the strains, SCB4, SCB6, and SCB7, compared with the SCB5 strain (Fig. 1). The shortest generation time of the SCB7 strain was 5 h, which was half that of the SCB5 strain (10 h). The genetic structures of the xylose-assimilating strains (SCB4, SCB6, and SCB7), *loxP*–P_{TEF}–*kanMX*–T_{TEF}–P_{TDH3}–*XYL1*–T_{TDH3}–P_{TDH3}–*XYL2*–T_{TDH3}–P_{TDH3}–*XKS1*–T_{TDH3}, were verified by PCR analysis and DNA sequencing. However, the PCR analysis and DNA sequencing of the SCB5 strain revealed that it had a deletion of *XKS1*.

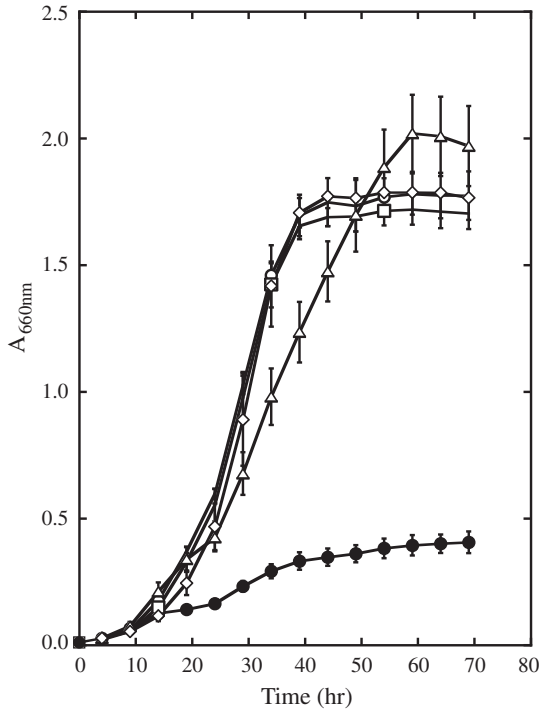

FIG. 1. Growth of xylose-assimilating *S. cerevisiae* SCB4, SCB5, SCB6, SCB7 and their parental strain SCA3. The cells of the five strains were inoculated into 5 mL of uracil-supplemented MSX medium (pH 5.5) containing 20 g/L xylose as the sole carbon source and incubated at 35°C with shaking. The cell density was monitored with the bio-photorecorder. The data presented are averages and standard deviations of three independently performed experiments. Open circles, SCB4; open triangles, SCB5; open squares, SCB6; open diamonds, SCB7; and closed circles, SCA3.

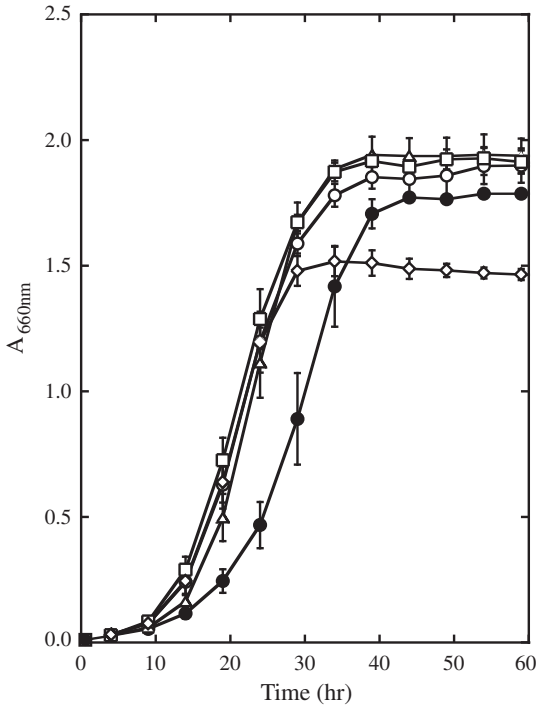

FIG. 2. Growth of *S. cerevisiae* Hex$^+$ mutants (SCB13, SCB14, SCB15, SCB16) and their parental strain SCB7. The cells of the five strains were inoculated into 5 mL of uracil-supplemented MSX medium (pH 5.5) containing 20 g/L xylose as the sole carbon source and incubated at 35°C with shaking. The cell density was monitored with the bio-photorecorder. The data presented are averages and standard deviations of three independently performed experiments. Open circles, SCB13; open triangles, SCB14; open squares, SCB15; open diamonds, SCB16; and closed circles, SCB7.

All of these observations indicated that one copy of *XYL1* and *XYL2* was sufficient for xylose assimilation in the SCA3 industrial *S. cerevisiae* genetic background. The addition of the endogenous *XKS1* (encoding *S. cerevisiae* xylulokinase) with the *TDH3* promoter allowed efficient aerobic growth (the shortest generation time of 5 h) in 20 g/L xylose as the sole carbon source compared with other strains reported thus far (43).

Isolation of mutants showing high efficiency of xylose assimilation (Hex$^+$ mutants) The development of xylose utilization by *S. cerevisiae* is important with respect to ethanol production. Hence, we isolated mutants from *S. cerevisiae* SCB7 with high efficiency of xylose assimilation. The strain SCB7 was cultivated in the uracil-supplemented MSX medium containing xylose as the sole carbon source at 35°C with shaking, and four mutants showing rapid growth were independently isolated (SCB13, SCB14, SCB15, and SCB16). The xylose assimilation of these four strains and their parental strain (SCB7) was analyzed by cultivating the cells in 5 mL of MSX medium (pH 5.5) at 35°C. The four mutants showed remarkably high efficient growth compared with their parental strain (SCB7) (Fig. 2). The shortest generation time of the SCB14 strain was 2.5 h, which was half that observed for the SCB7 strain (5 h). Because the mutants showed remarkably high assimilation of xylose, which was the sole carbon source, we tentatively designated the mutants as the high efficiency of xylose assimilation (Hex$^+$) mutants.

Genetic analysis of the Hex$^+$ mutants We performed the following genetic analyses of the Hex$^+$ mutants: (i) the number of the mutations included in the four mutants, (ii) the dominance of the mutations compared with the wild type allele, and (iii) the linkage relationship between the mutations. A diploid obtained from the cross between the Hex$^+$ mutant SCB14 (*MAT**a** pho87Δ ura3Δ*::XM_8 Hex_{2-2}) and the wild type Hex$^-$ strain SCB103-10D (*MATα ura3Δ*::XM_8) was sporulated, and the spore clones segregated 2 Hex$^+$:2 Hex$^-$ in 24 asci. The typical cell growth pattern in the uracil-supplemented MSX medium (pH 5.5) at 35°C was shown in Fig. 3a. When the other diploids from the crosses between the Hex$^+$ mutants (SCB13, SCB15 and SCB16) and the wild type Hex$^-$ strain SCB103-10D were analyzed, the same 2$^+$:2$^-$ segregations were also shown for Hex$^+$:Hex$^-$ in 30 asci, 24 asci, and 30 asci (growth patterns not shown). All of these observations indicated that each of the Hex$^+$ mutants had one mutation.

To analyze whether the four mutations were dominant to the wild type allele, the cell growth of the diploid hybrids obtained from the crosses between the four Hex$^+$ mutants (SCB13–SCB16) and the wild type Hex$^-$ strain (SCB103-10D; *MATα ura3Δ*::XM_8) were analyzed in uracil-supplemented MSX medium (pH 5.5) at 35°C. The cell growth of the diploid hybrid SCB104 that resulted from the strains SCB13 and SCB103-10D was similar to that of the wild type Hex$^-$ diploid strain SCB112 (Fig. 3b), indicating that the hex_{1-5} mutation of the strain SCB13 was recessive. The other three diploid hybrids showed rapid cell growth that was similar to that of the Hex$^+$ mutants (Fig. 3c–e). Hence, the three mutations of the strains SCB14, SCB15, and SCB16 were dominant, and we designated the three mutations as HEX_{2-2}, HEX_{2-3}, and HEX_{2-9}, respectively.

To detect the linkage relationship among the hex_{1-5}, HEX_{2-2}, HEX_{2-3}, and HEX_{2-9} mutations, the mutants were crossed in several combinations ($HEX_{2-2} \times HEX_{2-9}$, $HEX_{2-2} \times HEX_{2-3}$, $HEX_{2-2} \times hex_{1-5}$, and $hex_{1-5} \times HEX_{2-3}$). The diploid SCB113, which was obtained from the cross between the HEX_{2-2} mutant SCB105-3A and the HEX_{2-9} mutant SCB107-8D, was sporulated, and the spores segregated 4$^+$:0$^-$ for Hex$^+$:Hex$^-$ in 16 asci. The other diploids obtained from the crosses ($HEX_{2-2} \times HEX_{2-3}$, strain SCB114;

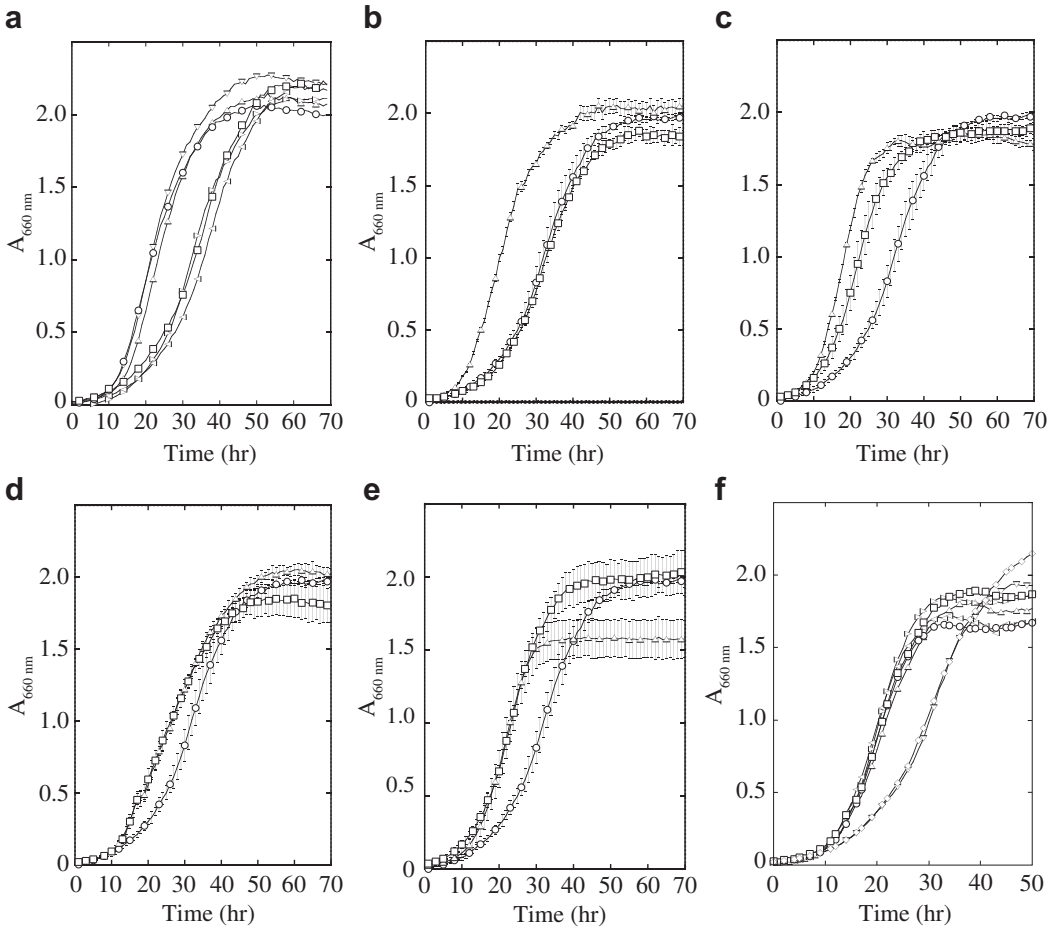

FIG. 3. Genetic analysis of *S. cerevisiae* Hex^+ mutants (SCB13, SCB14, SCB15, SCB16). The cells were inoculated into 5 mL of uracil-supplemented MSX medium (pH 5.5) containing 20 g/L xylose as the sole carbon source and incubated at 35°C with shaking. The cell density was monitored with the bio-photorecorder. (a) Analysis of four Hex^+ mutants. Cell growth of tetrads obtained from the cross between the Hex_{2-2} mutant (SCB14) and the wild type Hex^- strain (SCB103-10D), and its parental strains were analyzed. Open circles, SCB14; open squares, SCB103-10D; and the 4 spores of a single tetrad: open triangles, SCB105-5A; open downward triangles, SCB105-5B; open rightward triangles, SCB105-5C; and open leftward triangles, SCB105-5D. (b–e) Dominance test of hex_{1-5} (b), HEX_{2-2} (c), HEX_{2-3} (d), and HEX_{2-9} (e) mutations relative to the wild type allele. Open circles, *HEX/HEX* diploid strain (SCB112); open triangles, Hex^+/Hex^+ diploid strains (SCB108, SCB109, SCB110, and SCB111); open squares, Hex^+/Hex^- diploid hybrids (SCB104, SCB105, SCB106, and SCB107). (f) Allelism test. The HEX_{2-2} mutant SCB105-3A, HEX_{2-3} mutant SCB106-8D, wild type Hex^- strain SCB103-10D, and a tetrad of spores SCB114-5A, 5B, 5C, and 5D obtained from the cross between the HEX_{2-2} mutant SCB105-3A and HEX_{2-3} mutant SCB106-8D were analyzed. Circles, SCB105-3A; rectangles, SCB106-8D; diamonds, SCB103-10D; and the four spores of a tetrad: triangles, SCB114-5A; downward triangles, SCB114-5B; rightward triangles, SCB114-5C; and leftward triangles, SCB114-5D. (b–f) The data are averages and standard deviations of at least two independently performed experiments.

$HEX_{2-2} \times hex_{1-5}$, strain SCB115; $hex_{1-5} \times HEX_{2-3}$, strain SCB116) were sporulated. The occurrences of $4^+:0^-$, $3^+:1^-$, and $2^+:2^-$ segregations for $Hex^+:Hex^-$ for these tetrads were 2:8:1, 3:4:1, and 2:4:2 in 11 asci, 8 asci, and 8 asci, respectively. The typical cell growth pattern of tetrads obtained from the diploid SCB114 with $3^+:1^-$ segregation in the uracil-supplemented MSX medium (pH 5.5) at 35°C was shown in Fig. 3f. All of our observations indicated that the hex_{1-5}, HEX_{2-2}, and HEX_{2-3} mutations were not linked with each other and segregated independently; the HEX_{2-2} and HEX_{2-9} mutations were closely linked. Hence, we tentatively designated the HEX_{2-2} or HEX_{2-9} mutant gene as *HEX1*, the HEX_{2-3} mutant gene as *HEX2*, and the hex_{1-5} mutant gene as *hex3*.

Analysis of *hex3* and linkage analysis of *HEX1* and *HEX2* to *TAL1* Deletion of *PHO13* or overexpression of *TAL1* indicates an improvement of the growth on D-xylose (44,45). Hence we analyzed whether the *pho13Δ*::*kanMX* or P_{TDH3}–*TAL1* in the SCB7 genetic background showed the Hex^+ phenotype. The strain SCB44 (P_{TDH3}–*TAL1*) and SCB45 (*pho13Δ*::*kanMX*) strains were constructed and cultivated in the MSX medium (pH 5.5) at 35°C with shaking. The two strains showed the Hex^+ phenotype (Fig. 4a). To confirm the *pho13Δ*::*kanMX* mutation was recessive, the cell growth of the diploid hybrid SCB52 obtained from the cross between the *pho13Δ* strain (SCB45) and the wild type strain (SCB103-10D) was analyzed in the MSX medium (pH 5.5) at 35°C. The cell growth of the diploid strain SCB52 was similar to that of the wild type diploid strain SCB112, indicating that the *pho13Δ*::*kanMX* was recessive (Fig. 4b). To analyze whether the $hex3_{1-5}$ mutant allele was in the *PHO13*, we crossed the $hex3_{1-5}$ mutant with the *pho13Δ*::*kanMX* strain and tested the growth in the xylose minimal medium (MSX medium, pH 5.5) at 35°C. The diploid hybrid SCB49 (*pho13Δ*::*kanMX*/$hex3_{1-5}$) showed rapid growth that was similar to that of the Hex^+ mutants (Fig. 4b). Hence, the *hex3* gene was the *PHO13* gene.

To analyze the linkage relationship of *TAL1* to the *HEX1* and *HEX2*, the P_{TDH3}–*TAL1* strain SCB44 was crossed with the $HEX1_{2-2}$ strain SCB105-7A and the $HEX1_{2-3}$ strain SCB106-1D. The resultant diploid hybrids SCB47 and SCB48 were sporulated. The occurrences of $4^+:0^-$, $3^+:1^-$, and $2^+:2^-$ segregations for $Hex^+:Hex^-$ for these tetrads were 2:18:6 and 5:17:8 in 26 and 30 asci, respectively. The typical cell growth patterns of tetrads obtained from the diploids SCB47 and SCB48 with $2^+:2^-$ and $3^+:1^-$ segregations in the uracil-

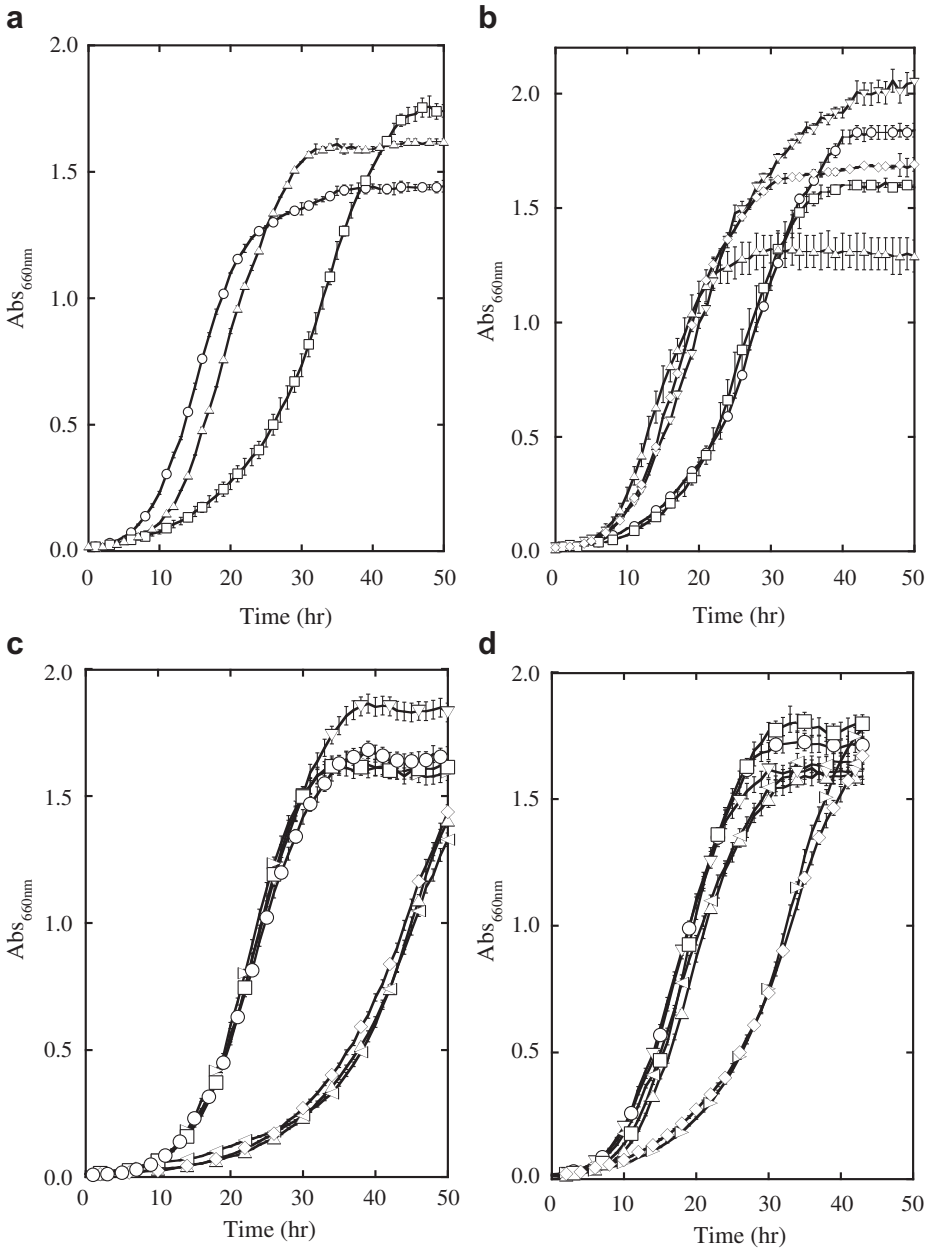

FIG. 4. Analysis of *S. cerevisiae pho13Δ* and P_{TDH3}—*TAL1* strains for the Hex^+ phenotype, and linkage analysis of the *HEX1* and *HEX2* to the *TAL1* gene. The cells were inoculated into 5 mL of MSX medium (pH 5.5) containing 20 g/L xylose as the sole carbon source and incubated at 35°C with shaking. The cell density was monitored with the bio-photorecorder. (a) Analysis of *pho13Δ*, P_{TDH3}—*TAL1*, and wild type strain. Squares, SCC2-11B (wild type); circles, SCB45 (*pho13Δ*); and triangles, SCB44 (P_{TDH3}—*TAL1*). (b) Dominance test of *pho13Δ* and complementation test between $hex3_{1-5}$ and *pho13Δ*. Circles, Hex^-/Hex^- diploid strain (SCB112); triangles, *pho13Δ/pho13Δ* diploid strain (SCB53); squares, *pho13Δ*/Hex^- diploid hybrids (SCB52); downward triangles, $hex3_{1-5}$/$hex3_{1-5}$ diploid strain (SCB108), and diamonds, *pho13Δ*/$hex3_{1-5}$ diploid hybrids (SCB49). (c) Linkage analysis of $HEX1_{2-2}$ to the *TAL1* gene. Cell growth of tetrads obtained from the cross between the $HEX1_{2-2}$ mutant (SCB105-7A) and the P_{TDH3}-*TAL1* strain (SCB44), and the Hex^- strain (SCC2-11B) were analyzed. Circles, SCB44; squares, SCB105-7A; the 4 spores of a single tetrad: triangles, SCB47-3A; downward triangles, SCB47-3B; rightward triangles, SCB47-3C; and leftward triangles, SCB47-3D; and diamonds, SCC2-11B. (d) Linkage analysis of $HEX1_{2-3}$ to the *TAL1* gene. Cell growth of tetrads obtained from the cross between the $HEX1_{2-3}$ mutant (SCB106-1D) and the P_{TDH3}-*TAL1* strain (SCB44), and the Hex^- strain (SCC2-11B) were analyzed. Circles, SCB44; squares, SCB106-1D; the 4 spores of a single tetrad: triangles, SCB48-6A; downward triangles, SCB48-6B; rightward triangles, SCB48-6C; and leftward triangles, SCB48-6D; and diamonds, SCC2-11B. (a—d) The data are averages and standard deviations of at least three independently performed experiments.

supplemented MSX medium (pH 5.5) at 35°C were shown in Fig. 4c and d. All of the observations indicated that *TAL1* was not linked with *HEX1* and *HEX2*, and the three genes were different with each other.

Batch fermentation The four Hex^+ mutants (SCB14—SCB16) and their parental strain (SCB7) were used for the batch fermentation in YPX medium (pH 4.0) containing 30 g/L xylose at 35°C with shaking (60 rpm) and an initial cell density (A_{660}) of 1.0. All of the Hex^+ mutants grew rapidly with increasing cultivation time, but the SCB7 parental strain showed growth retardation at the early phase of cultivation (Fig. 5a). The xylose consumption and ethanol production were similar to the growth results (Fig. 5b and c). From the $HEX1_{2-2}$ mutant, 4.8 g/L ethanol was produced within 24 h, which was 1.4 times higher than that achieved by the parental strain at 24 h (3.4 g/L ethanol). The ethanol yield of the $HEX1_{2-2}$ mutant was 47%. The ethanol production and yield of the $HEX2_{2-3}$ mutant were similar to those of the $HEX1_{2-2}$ mutant. The xylose concentrations in the

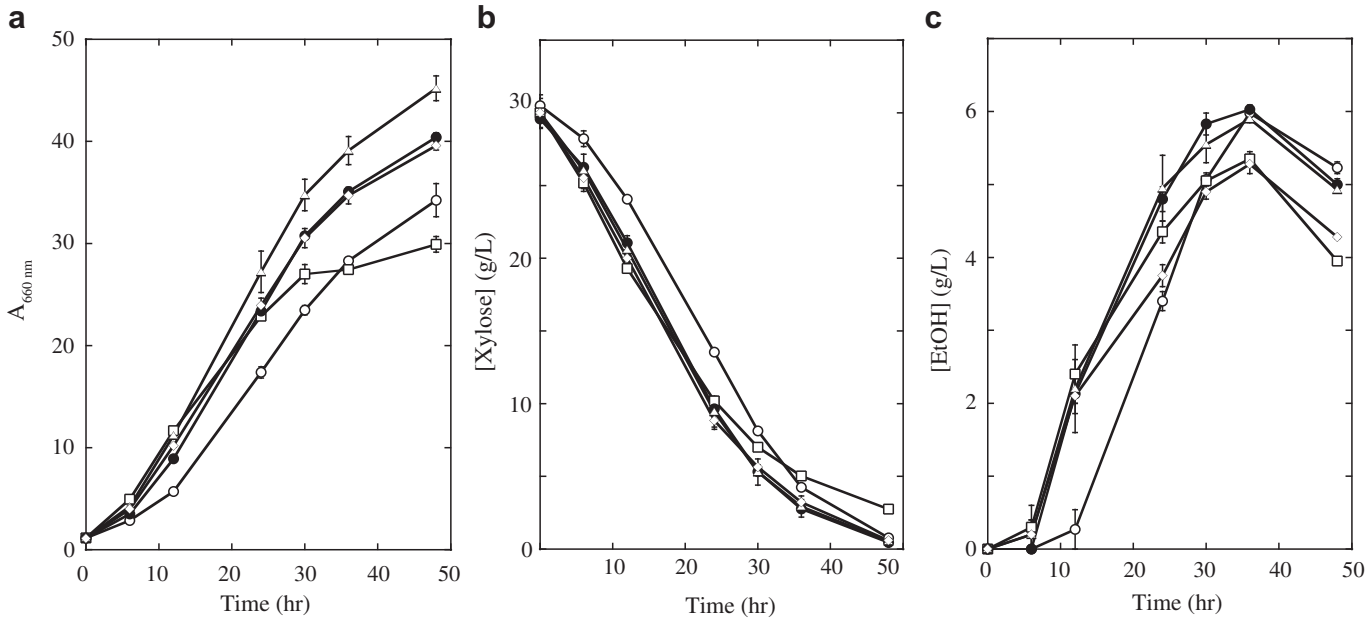

FIG. 5. Batch fermentation of *S. cerevisiae* Hex^+ mutants (SCB13, SCB14, SCB15, and SCB16) and their parental strain SCB7. The cells of the five strains were fermented in 50 mL of YPX medium (pH 4.0) containing 30 g/L xylose as the sole carbon source and incubated at 35°C with shaking. The cell density, xylose concentration, and alcohol concentration were analyzed. The data presented are averages and standard deviations of three independently performed experiments. Open circles, SCB7; open squares, SCB13; closed circles, SCB14; open triangles, SCB15; open diamonds, SCB16. (a) Cell growth ($A_{660\ nm}$); (b) xylose concentration (g/L); and (c) ethanol concentration (g/L).

medium for each of the four Hex^+ mutants linearly decreased at a rate of 1 g/L/hr until 24 h. These results indicated that the *HEX1*, *HEX2*, and *hex3* mutations resulted inefficient xylose consumption, and ethanol production began at the beginning of fermen tation.

DISCUSSION

The thermotolerant and acid tolerant *S. cerevisiae* NAM34-4C strain with potent lactic acid assimilation and high transformability was developed from the industrial *S. cerevisiae* KF7 strain that was used for fuel ethanol production. From the NAM34-4C strain, we constructed the isogenic strains SCA3 (*MAT**a** pho87Δ*) and SCA2 (*MATα*). As the draft DNA sequence information of the NAM34-4C strain could be obtained (unpublished result), we could easily, accurately, and isogenically analyze and improve the strains by standard yeast genetics and gene manipulations based on genome information. The xylose assimilation ability of the SCB7 strain, which was derived from the SCA3 and carried one copy of *XYL1*, *XYL2*, and the endogenous *XKS1* gene under the control of *TDH3* promoter in the chromosomal DNA, was very high compared with other strains that have been published (43,46,47). The sufficient efficiency of xylose assimilation might be derived from the properties of the industrial ethanol producing strain KF7, which showed thermotolerance, acid tolerance, potent lactate assimilation, and other stress tolerance.

Four *HEX* mutations were classified into three linkage groups: $HEX1_{2-2}$ and $HEX1_{2-9}$; $HEX2_{2-3}$; $hex3_{1-5}$. Possible combinations of the double mutations, $HEX1_{2-2}$ and $HEX2_{2-3}$, $HEX1_{2-2}$ and $hex3_{1-5}$, and $HEX2_{2-3}$ and $hex3_{1-5}$, did not show additive or synergistic effects on xylose assimilation compared with the single mutant (MSX medium, pH 5.5 at 35°C: $G_{short} = 2.5$ h). Hence, other mutations were necessary for superior xylose assimilation ability that approached that of glucose assimilation.

Pho13 possessed *p*-nitrophenyl phosphatase activity against phosphorylated proteins, particularly histones (44,45,48) and casein (48). The *pho13Δ* mutation in the *S. cerevisiae* CMB.JHV. XYL123.pho13a (44) and in the SCB45 (Fig. 4a) led to improved growth and ethanol production on D-xylose. As the $hex3_{1-5}$ leading to C31Y amino acid substitution (unpublished result) was the *PHO13* gene (Fig. 4b), the deficient Pho13 (C31Y) as well as the lack of the Pho13 possibly played the same role in the xylose assimilation; namely, regulatory effects of the phosphatase (45).

Overexpression of *TAL1* in *S. cerevisiae* L2612 (pYES2-X123 and pRS314−ADHtal) (45) and SCB44 (Fig. 4a) led to improved growth and ethanol production on D-xylose. However the *TAL1* was different from the two dominant *HEX1* and *HEX2* mutant genes. As the overexpression of the *TAL1* is most likely needed for large-scale replacement of *TAL1* promoter, for example, with *ADH3* (47), *PGK1* (48,49) or *TDH3* promoter, *TAL1* up-promoter mutant was not likely selected in the four Hex mutants. The identification of the $HEX1_{2-2}$ and $HEX2_{2-3}$ mutant genes using the sequencing by oligonucleotide ligation and detection (SOLiD) next-generation sequencing system and the characterization of the mutations are currently underway.

The batch fermentation of recombinant *S. cerevisiae* and the Hex mutants was carried out in YPX3 medium with xylose as the sole carbon source. Then, the ethanol concentration in the medium with the Hex mutants increased with a decrease in the xylose concentration (Fig. 5). When the xylose consumption of recombinant *S. cerevisiae* was slow during the early phase of cultivation, ethanol production was very low. Thus, the xylose consumption and ethanol production were interlocked. Because the cell growth increased with increased xylose consumption, we speculated that higher ethanol productivity would be derived from increased cell growth through increased xylose consumption.

Ethanol yields (47%) of the four Hex mutants were relatively low compared with other strains that have been published (30,50). However, the yield is dependent on fermentation conditions; for example, temperature, pH value, initial cell density, culture media, shaking speed, shaking type (rotatory or reciprocal), culture bottles equipped with or without a bubbling CO_2 outlet. Although we did not carry out the ethanol fermentation at the optimal condition,

ethanol yield of the *HEX1*$_{2-2}$ mutant increased 54% at 30°C in our condition (unpublished result).

Supplementary data associated with this article can be found in online version at http://dx.doi.org/10.1016/j.jbiosc.2013.05.027.

ACKNOWLEDGMENTS

We acknowledge Dr. S. Harashima (Department of Biotechnology, Graduate School of Engineering, Osaka University) for kindly providing the pSH47 plasmid, and the *S. cerevisiae* S288C and SH6710 strains. We thank Dr. A. Kondo (Department of Chemical Science and Engineering, Graduate School of Engineering, Kobe University) for kindly providing the *S. cerevisiae* KF7M strain. This work was supported in part by the New Energy and Industrial Technology Development Organization (NEDO) and Grants-in-Aid for a greenhouse gas mitigation technology development program from the Ministry of the Environment of Japan.

References

1. **Zhang, X. Y., Yu, H. B., Huang, H. Y., and Liu, Y. X.:** Evaluation of biological pretreatment with white rot fungi for the enzymatic hydrolysis of bamboo culms, Int. Biodeterior. Biodegradation, **60**, 159–164 (2007).
2. **Shimokawa, T., Ishida, M., Yoshida, S., and Nojiri, M.:** Effects of growth stage on enzymatic saccharification and simultaneous saccharification and fermentation of bamboo shoots for bioethanol production, Bioresour. Technol., **100**, 6651–6654 (2009).
3. **Yamashita, Y., Shono, M., Sasaki, C., and Nakamura, Y.:** Alkaline peroxide pretreatment for efficient enzymatic saccharification of bamboo, Carbohydr. Polym., **79**, 914–920 (2010).
4. **Sun, Y. and Lin, L.:** Hydrolysis behavior of bamboo fiber in formic acid reaction system, J. Agric. Food Chem., **58**, 2253–2259 (2010).
5. **Sun, Z. Y., Tang, Y. Q., Iwanaga, T., Sho, T., and Kida, K.:** Production of fuel ethanol from bamboo by concentrated sulfuric acid hydrolysis followed by continuous ethanol fermentation, Bioresour. Technol., **102**, 10929–10935 (2011).
6. **Batt, C. A., Carvallo, S., Easson, D. D., Akedo, M., and Sinskey, A. J.:** Direct evidence for a xylose metabolic pathway in *Saccharomyces cerevisiae*, Biotechnol. Bioeng., **28**, 549–553 (1986).
7. **van Zyl, C., Prior, B. A., Kilian, S. G., and Kock, J. L.:** D-Xylose utilization by *Saccharomyces cerevisiae*, J. Gen. Microbiol., **135**, 2791–2798 (1989).
8. **Kruckeberg, A. L.:** The hexose transporter family of *Saccharomyces cerevisiae*, Arch. Microbiol., **166**, 283–292 (1996).
9. **Bisson, L. F., Coons, D. M., Kruckeberg, A. L., and Lewis, D. A.:** Yeast sugar transporters, Crit. Rev. Biochem. Mol. Biol., **28**, 259–308 (1993).
10. **Boles, E. and Hollenberg, C. P.:** The molecular genetics of hexose transport in yeasts, FEMS Microbiol. Rev., **21**, 85–111 (1997).
11. **Lee, W. J., Kim, M. D., Ryu, Y. W., Bisson, L. F., and Seo, J. H.:** Kinetic studies on glucose and xylose transport in *Saccharomyces cerevisiae*, Appl. Microbiol. Biotechnol., **60**, 186–191 (2002).
12. **Hamacher, T., Becker, J., Gardonyi, M., Hahn-Hägerdal, B., and Boles, E.:** Characterization of the xylose-transporting properties of yeast hexose transporters and their influence on xylose utilization, Microbiology, **148**, 2783–2788 (2002).
13. **Busturia, A. and Lagunas, R.:** Catabolite inactivation of the glucose transport system in *Saccharomyces cerevisiae*, J. Gen. Microbiol., **132**, 379–385 (1986).
14. **Diderich, J. A., Schepper, M., van Hoek, P., Luttik, M. A., van Dijken, J. P., Pronk, J. T., Klaassen, P., Boelens, H. F. M., de Mattos, J. T., van Dam, K., and Kruckeberg, A. L.:** Glucose uptake kinetics and transcription of *HXT* genes in chemostat cultures of *Saccharomyces cerevisiae*, J. Biol. Chem., **274**, 15350–15359 (1999).
15. **Webb, S. R. and Lee, H.:** Regulation of D-xylose utilization by hexoses in pentose-fermenting yeasts, Biotechnol. Adv., **8**, 685–697 (1990).
16. **Hahn-Hägerdal, B., Linden, T., Senac, T., and Skoog, K.:** Ethanolic fermentation of pentoses in lignocellulose hydrolysates, Appl. Biochem. Biotechnol., **28–29**, 131–144 (1991).
17. **Aristidou, A. and Penttila, M.:** Metabolic engineering applications to renewable resource utilization, Curr. Opin. Biotechnol., **11**, 187–198 (2000).
18. **Eliasson, A., Christensson, C., Wahlbom, C. F., and Hahn-Hägerdal, B.:** Anaerobic xylose fermentation by recombinant *Saccharomyces cerevisiae* carrying *XYL1*, *XYL2*, and *XKS1* in mineral medium chemostat cultures, Appl. Environ. Microbiol., **66**, 381–3386 (2000).
19. **Kotter, P. and Ciriacy, M.:** Xylose fermentation by *Saccharomyces cerevisiae*, Appl. Microbiol. Biotechnol., **38**, 776–783 (1993).
20. **Bruinenberg, P. M., Debot, P. H. M., Vandijken, J. P., and Scheffers, W. A.:** NADH linked aldose reductase – the key to anaerobic alcoholic fermentation of xylose by yeasts, Appl. Microbiol. Biotechnol., **19**, 256–260 (1984).
21. **Walfridsson, M., Hallborn, J., Penttila, M., Keranen, S., and Hahn-Hägerdal, B.:** Xylose-metabolizing *Saccharomyces cerevisiae* strains overexpressing the *TKL1* and *TAL1* genes encoding the pentose phosphate pathway enzymes transketolase and transaldolase, Appl. Environ. Microbiol., **61**, 4184–4190 (1995).
22. **Boles, E., Lehnert, W., and Zimmermann, F. K.:** The role of the NAD dependent glutamate dehydrogenase in restoring growth on glucose of a *Saccharomyces cerevisiae* phosphoglucose isomerase mutant, Eur. J. Biochem., **217**, 469–477 (1993).
23. **Muller, S., Boles, E., May, M., and Zimmermann, F. K.:** Different internal metabolites trigger the induction of glycolytic gene-expression in *Saccharomyces cerevisiae*, J. Bacteriol., **177**, 4517–4519 (1995).
24. **Gardonyi, M., Jeppsson, M., Liden, G., Gorwa-Grauslund, M. F., and Hahn-Hägerdal, B.:** Control of xylose consumption by xylose transport in recombinant *Saccharomyces cerevisiae*, Biotechnol. Bioeng., **82**, 818–824 (2003).
25. **Grotkjaer, T., Christakopoulos, P., Nielsen, J., and Olsson, L.:** Comparative metabolic network analysis of two xylose fermenting recombinant *Saccharomyces cerevisiae* strains, Metab. Eng., **7**, 437–444 (2005).
26. **Krahulec, S., Klimacek, M., and Nidetzky, B.:** Analysis and prediction of the physiological effects of altered coenzyme specificity in xylose reductase and xylitol dehydrogenase during xylose fermentation by *Saccharomyces cerevisiae*, J. Biotechnol., **158**, 192–202 (2012).
27. **Petschacher, B. and Nidetzky, B.:** Altering the coenzyme preference of xylose reductase to favor utilization of NADH enhances ethanol yield from xylose in a metabolically engineered strain of *Saccharomyces cerevisiae*, Microb. Cell Fact., **7**, 9 (2008).
28. **Watanabe, S., Saleh, A. A., Pack, S. P., Annaluru, N., Kodaki, T., and Makino, K.:** Ethanol production from xylose by recombinant *Saccharomyces cerevisiae* expressing protein-engineered NADH-preferring xylose reductase from *Pichia stipitis*, Microbiology, **153**, 3044–3054 (2007).
29. **Watanabe, S., Kodaki, T., and Makino, K.:** Complete reversal of coenzyme specificity of xylitol dehydrogenase and increase of thermostability by the introduction of structural zinc, J. Biol. Chem., **280**, 10340–10349 (2005).
30. **Ismail, K. S. K., Sakamoto, T., Hatanaka, H., Hasunuma, T., and Kondo, A.:** Gene expression cross-profiling in genetically modified industrial *Saccharomyces cerevisiae* strains during high-temperature ethanol production from xylose, J. Biotechnol., **163**, 50–60 (2012).
31. **Sanda, T., Hasunuma, T., Matsuda, F., and Kondo, A.:** Repeated-batch fermentation of lignocellulosic hydrolysate to ethanol using a hybrid *Saccharomyces cerevisiae* strain metabolically engineered for tolerance to acetic and formic acids, Bioresour. Technol., **102**, 7917–7924 (2011).
32. **Sonderegger, M. and Sauer, U.:** Evolutionary engineering of *Saccharomyces cerevisiae* for anaerobic growth on xylose, Appl. Environ. Microbiol., **69**, 1990–1998 (2003).
33. **Pitkanen, J. P., Rintala, E., Aristidou, A., Ruohonen, L., and Penttila, M.:** Xylose chemostat isolates of *Saccharomyces cerevisiae* show altered metabolite and enzyme levels compared with xylose, glucose, and ethanol metabolism of the original strain, Appl. Microbiol. Biotechnol., **67**, 827–837 (2005).
34. **Attfield, P. V. and Bell, P. J.:** Use of population genetics to derive nonrecombinant *Saccharomyces cerevisiae* strains that grow using xylose as a sole carbon source, FEMS Yeast Res., **6**, 862–868 (2006).
35. **Wakamatsu, M., Tani, T., Taguchi, H., Matsuoka, M., Kida, K., and Akamatsu, T.:** Ethanol production from D-lactic acid by lactic acid-assimilating *Saccharomyces cerevisiae* NAM34-4C, J. Biosci. Bioeng., **116**, 85–90 (2013).
36. **Güldener, U., Heck, S., Fielder, T., Beinhauer, J., and Hegemann, J. H.:** A new efficient gene disruption cassette for repeated use in budding yeast, Nucleic Acids Res., **24**, 2519–2524 (1996).
37. **Takeno, M., Taguchi, H., and Akamatsu, T.:** Role of ComFA in controlling the DNA uptake rate during transformation of competent *Bacillus subtilis*, J. Biosci. Bioeng., **111**, 618–623 (2011).
38. **Maniatis, T., Fritsch, E. F., and Sambrook, J.:** Molecular cloning, a laboratory manual. Cold Spring Harbor Laboratory, Cold Spring Harbor, NY (1982).
39. **Gietz, R. D. and Woods, R. A.:** Transformation of yeast by lithium acetate/single-stranded carrier DNA/polyethylene glycol method, Methods Enzymol., **350**, 87–96 (2002).
40. **Sherman, F., Fink, G. R., and Hicks, J. B.:** Laboratory course manual for methods in yeast genetics. Cold Spring Harbor Laboratory Press, Cold Spring Harbor, NY (1989).
41. **Birnboim, H. C. and Doly, J.:** A rapid alkaline extraction procedure for screening recombinant plasmid DNA, Nucleic. Acids Res., **7**, 1513–1523 (1979).
42. **Alting-Mees, M. A. and Short, J. M.:** pBluescript II: gene mapping vectors, Nucleic Acids Res., **17**, 9494 (1989).
43. **Chu, B. C. H. and Lee, H.:** Genetic improvement of *Saccharomyces cerevisiae* for xylose fermentation, Biotechnol. Adv., **25**, 425–441 (2007).
44. **Van Vleet, J. H., Jeffries, T. W., and Olsson, L.:** Deleting the para-nitrophenyl phosphatase (pNPPase), *PHO13*, in recombinant *Saccharomyces cerevisiae* improves growth and ethanol production on D-xylose, Metab. Eng., **10**, 360–369 (2008).

45. **Ni, H., Laplaza, J. M., and Jeffries, T. W.:** Transposon mutagenesis to improve the growth of recombinant *Saccharomyces cerevisiae* on D-xylose, Appl. Environ. Microbiol., **73**, 2061–2066 (2007).
46. **Runquist, D., Hahn-Hägerdal, B., and Bettiga, M.:** Increased ethanol productivity in xylose-utilizing *Saccharomyces cerevisiae* via a randomly mutagenized xylose reductase, Appl. Environ. Microbiol., **76**, 7796–7802 (2010).
47. **Olofsson, K., Runquist, D., Hahn-Hägerdal, B., and Lidén, G.:** A mutated xylose reductase increases bioethanol production more than a glucose/xylose facilitator in simultaneous fermentation and co-fermentation of wheat straw, AMB Express, **1**, 4 (2011).
48. **Tuleva, B., Vasileva-Tonkova, E., and Galabova, D.:** A specific alkaline phosphatase from *Saccharomyces cerevisiae* with protein phosphatase activity, FEMS Microbiol. Lett., **161**, 139–144 (1998).
49. **Hasunuma, T., Sanda, T., Yamada, R., Yoshimura, K., Ishii, J., and Kondo, A.:** Metabolic pathway engineering based on metabolomics confers acetic and formic acid tolerance to a recombinant xylose-fermenting strain of *Saccharomyces cerevisiae*, Microb. Cell Fact., **10**, 2 (2011).
50. **Katahira, S., Mizuike, A., Fukuda, H., and Kondo, A.:** Ethanol fermentation from lignocellulosic hydrolysate by a recombinant xylose- and cellooligosaccharide-assimilating yeast strain, Appl. Microbiol. Biotechnol., **72**, 1136–1143 (2006).